# Improved constraints on exotic electron-proton interactions in hydrogen

Lei Cong [1,2,3] Filip Ficek [4,5] Pavel Fadeev [3] and Dmitry Budker [1,2,3,6,*]

[1] *Helmholtz Institute Mainz, 55099 Mainz, Germany*
[2] *GSI Helmholtzzentrum für Schwerionenforschung GmbH, 64291 Darmstadt, Germany*
[3] *Johannes Gutenberg University, Mainz 55128, Germany*
[4] *Faculty of Mathematics, University of Vienna, Oskar-Morgenstern-Platz 1, 1090 Vienna, Austria*
[5] *Gravitational Physics Group, University of Vienna, Währinger Straße 17, 1090 Vienna, Austria*
[6] *Department of Physics, University of California at Berkeley, Berkeley, California 94720-7300, USA*

(Received 28 May 2025; accepted 17 October 2025; published 20 November 2025)

Atomic spectroscopy provides a sensitive tool for searching for new bosons that mediate exotic forces between elementary fermions. A comparison between a recent high-precision measurement [Bullis *et al.*, Phys. Rev. Lett. **130**, 203001 (2023)] of the hyperfine splitting of the $2S_{1/2}$ electronic level in hydrogen and up-to-date bound-state quantum electrodynamics calculations yields improved constraints on electron-proton exotic interactions. These are expressed in terms of the dimensionless coupling strengths $g_A g_A$, $g_p g_p$, and $g_V g_V$, corresponding to the exchange of axial-vector, pseudoscalar (axionlike), and vector bosons, respectively. Building on these results, our analysis highlights the importance of examining combinations of spin-dependent potentials that contribute to the same class of exotic interactions. In particular, we employ the combination $V_2 + V_3$ for both axial-vector–axial-vector and vector-vector couplings. These findings motivate further precision measurements toward spin-dependent exotic interactions.

DOI: 10.1103/8nyk-sysy

## I. INTRODUCTION

Precise experiments with atoms and molecules [1], together with other systems such as color centers in diamond [2], comagnetometers [3,4], and torsion pendulums [5], have been successfully employed to explore potential extensions to the Standard Model (SM), including searches for new particles. Various simple atomic systems [6–9], such as positronium, muonium, helium, antiprotonic helium, antihydrogen, and hydrogen, have been utilized to probe spin-dependent exotic interactions [10–14], with their sensitivity largely determined by advances in experimental and theoretical precision. Recently, a precision record [15] was set by a measurement of the hyperfine splitting of the $2S_{1/2}$ electronic levels of hydrogen. This breakthrough offers an opportunity to significantly improve upon previous constraints on spin-dependent exotic interactions between the electron and the proton [6,9].

Spin-dependent exotic interactions—interactions of a new boson with fermion spins—have attracted increasing interest in recent years [1,13]. Theoretical studies [10–12] show that such exotic potentials may arise from the exchange of either a spin-0 boson—such as the axion [16–21] and axionlike particles (ALPs) [22,23]—or a spin-1 boson, such as the $Z'$ boson [24] and the paraphoton $\gamma'$ [25–28]. These new bosons are among the leading candidates for addressing major open questions in fundamental physics, including the nature of dark matter [29–34] and the resolution of the strong charge-parity problem [35,36]. A spin-1 boson can mediate six types of interactions between fermions [13], depending on the vector (V), axial-vector (A), tensor (T), and pseudotensor ($\tilde{T}$) vertex combinations: $V$–$V$, $A$–$A$, $A$–$V$, $T$–$T$, $\tilde{T}$–$\tilde{T}$, and $\tilde{T}$–$T$. A spin-0 boson can couple to fermions through scalar ($s$) and pseudoscalar ($p$) channels, leading to three distinct interaction types: $s$–$s$, $p$–$p$, and $p$–$s$. While previous studies involving hydrogen [6,9] have constrained some of these interactions—specifically, the $A$-$A$ and $p$-$p$ types—the $V$-$V$ type of spin-dependent exotic interaction has not yet been accurately explored.

In this work, we make two advances. First, we improve the constraints on electron-proton exotic interactions. By comparing experimental data with up-to-date theoretical values from bound-state quantum electrodynamics, constraints on electron-proton exotic interactions can be obtained. Second, we study a previously [9] unconstrained type of exotic interaction between electron and proton—the vector-vector type—that can be probed via the hydrogen system. Although this interaction has largely been overlooked (for instance, existing constraints on $V_2$ and $V_3$ have not been interpreted in terms of vector-vector interactions), it merits equal attention based on the comprehensive theoretical framework recently summarized in Ref. [13].

## II. METHODS

### A. The hyperfine splitting difference $D_{21}$

The hyperfine splitting difference, $D_{21} = 8\Delta_{\rm hfs}(2S) - \Delta_{\rm hfs}(1S)$, is a critical parameter for probing the presence of

*Contact author: budker@uni-mainz.de

TABLE I. Comparison of theoretical and experimental values of $D_{21}$ used to calculate $\Delta D$.

| Parameter | $D_{21}$ Used in Ref. [9] | $D_{21}$ Used in this work |
|---|---|---|
| Theory (kHz) | 48.953(3) [43,44] | 48.9541(23) [40] |
| Expt. (kHz) | 48.923(54) [41,45] | 48.9592(68) [15] |
| $\mu$ (kHz) | 0.03 | −0.0051 |
| $\sigma$ (kHz) | 0.054 | 0.0072 |
| $\Delta D$ (kHz) (90%) | 0.102 | 0.0144 |

exotic forces in atomic physics. In conventional atoms, the sensitivity of tests based on the hyperfine structure (hfs) is limited by insufficient knowledge of their nuclear structure [37]. However, since the lowest-order nuclear corrections to $\Delta_{\rm hfs}(2S)$ and $\Delta_{\rm hfs}(1S)$ scale with the electron density in the ratio 1 : 8, they do not contribute to the difference $D_{21}$. Of course, some residual contributions to $D_{21}$ from nuclear structure and other standard-model effects [38–40] still apply. This provides a chance to test the quantum electrodynamics theory of bound states at a level of precision that is orders-of-magnitude better than that achievable for the ground-state hyperfine interval $\Delta_{\rm hfs}(1S)$ alone [41] and also offers a good opportunity for new physics searches. A similar specific difference defined for hydrogen- and lithiumlike highly charged ions was employed in Ref. [42] to cancel nuclear-structure contributions.

Recent experiments utilized Ramsey spectroscopy, rather than an optical frequency comb, to directly measure the $2S$ splitting, achieving the most precise determination of $D_{21}$ to date [15]. In the meantime, we identified improved theoretical results based on a direct, high-precision, all-order numerical calculation of the electron self-energy, with the uncertainty of $D_{21}$ being essentially dominated by the self-energy contribution [40]. The theoretical and experimental determinations of $D_{21}$ exhibit comparable precision and agree within the stated uncertainties.

Table I summarizes the current data concerning the value of $D_{21}$, in particular the results of theoretical calculations and experimental measurements, their difference $\mu$, and the combined uncertainty $\sigma = \sqrt{{\sigma_{\rm th}}^2 + {\sigma_{\rm expt}}^2}$. We use these to derive $\Delta D$, representing the maximal deviation at a 90% confidence level,

$$I = \int_{-\Delta D}^{\Delta D} \frac{1}{\sqrt{2\pi}\sigma} e^{-\frac{(x-\mu)^2}{2\sigma^2}} dx = 90\%. \tag{1}$$

The choice of a 90% confidence level allows us to compare the obtained constraints on the exotic interactions with previous results [6,8,9]. However, following the suggestion made in the review [13], we also present results at the 95%-confidence level (see Ref. [51]).

### B. Exotic potentials

By comparing the value of $\Delta D$ from Ref. [9] with our result in Table I, we find a sevenfold improvement. To illustrate how this improvement is related to the resulting constraints [see Eq. (11)] on the coupling constants, we first present the relevant exotic potentials.

The constraints on $g_p^e g_p^p$ and $g_A^e g_A^p$ were originally established by [9], based on $V_{AA}$ (i.e., $V2|_{AA} + V3|_{AA}$) and $V pp$ (i.e., $V3|_{pp}$).

$$V_2|_{AA} = -g_A^e g_A^p \frac{\hbar c}{4\pi} \boldsymbol{\sigma}_e \cdot \boldsymbol{\sigma}_p \frac{1}{r} e^{-r/\lambda}, \tag{2}$$

$$\begin{aligned} V_3|_{AA} = &-g_A^e g_A^p \frac{\hbar c}{4\pi} \lambda^2 \bigg[ \boldsymbol{\sigma}_e \cdot \boldsymbol{\sigma}_p \left[ \frac{1}{r^3} + \frac{1}{\lambda r^2} + \frac{4\pi}{3}\delta(\boldsymbol{r}) \right] \\ &- (\boldsymbol{\sigma}_e \cdot \hat{\boldsymbol{r}})(\boldsymbol{\sigma}_p \cdot \hat{\boldsymbol{r}}) \left( \frac{3}{r^3} + \frac{3}{\lambda r^2} + \frac{1}{\lambda^2 r} \right) \bigg] e^{-r/\lambda}, \end{aligned} \tag{3}$$

$$\begin{aligned} V_3|_{pp} = &-g_p^e g_p^p \frac{\hbar^3}{16\pi c} \frac{1}{m_e m_p} \bigg\{ \boldsymbol{\sigma}_e \cdot \boldsymbol{\sigma}_p \left[ \frac{1}{r^3} + \frac{1}{\lambda r^2} + \frac{4\pi}{3}\delta(\boldsymbol{r}) \right] \\ &- (\boldsymbol{\sigma}_e \cdot \hat{\boldsymbol{r}})(\boldsymbol{\sigma}_p \cdot \hat{\boldsymbol{r}}) \left( \frac{3}{r^3} + \frac{3}{\lambda r^2} + \frac{1}{\lambda^2 r} \right) \bigg\} e^{-r/\lambda}, \end{aligned} \tag{4}$$

where $\boldsymbol{\sigma}_e$ and $\boldsymbol{\sigma}_p$ are the Pauli vector operators corresponding to the spins $\boldsymbol{s}_i = \hbar\boldsymbol{\sigma}_i/2$ of the electron and proton; $\mathbf{r}$ denotes the difference of positions of the fermions, $r = |\mathbf{r}|$ is the distance between them, while $\hat{\mathbf{r}}$ is the unit vector in the direction of $\mathbf{r}$; $\lambda$ is the range of the force, given by $\lambda = \hbar/(Mc)$, where $M$ is the mass of the new boson; and $m_e$ and $m_p$ represent the masses of the electron and proton, respectively.

We further emphasize that the vector-vector interaction described by $(V_2 + V_3)|_{VV}$ [13] can and should also be explored within the framework. This exotic potential has the form

$$\begin{aligned} &(V_2 + V_3)|_{VV} \\ &= g_V^e g_V^p \frac{\hbar^3}{16\pi c m_e m_p} \bigg\{ \boldsymbol{\sigma}_e \cdot \boldsymbol{\sigma}_p \left[ \frac{1}{r^3} + \frac{1}{\lambda r^2} + \frac{1}{\lambda^2 r} - \frac{8\pi}{3}\delta(\boldsymbol{r}) \right] \\ &\quad - (\boldsymbol{\sigma}_e \cdot \hat{\boldsymbol{r}})(\boldsymbol{\sigma}_p \cdot \hat{\boldsymbol{r}}) \left( \frac{3}{r^3} + \frac{3}{\lambda r^2} + \frac{1}{\lambda^2 r} \right) \bigg\} e^{-r/\lambda}. \end{aligned} \tag{5}$$

### C. Exotic contribution to the hyperfine splitting difference

The exchange of a new boson via exotic interaction potentials can lead to measurable shifts in atomic spectroscopy. To estimate these energy shifts, we use the hydrogenic wave functions for the $1S$ and $2S$ states to evaluate the contribution of a given potential $V_i$ to the hfs. The resulting exotic contribution to the differential HFS interval is defined as

$$\Delta E_{D_{21}}^{\rm Exotic} = 8\Delta E_{2S}^{\rm hfs} - \Delta E_{1S}^{\rm hfs}, \tag{6}$$

where

$$\Delta E_{nS}^{\rm hfs} = \langle \psi_{nS}^{F=1} | V_i | \psi_{nS}^{F=1} \rangle - \langle \psi_{nS}^{F=0} | V_i | \psi_{nS}^{F=0} \rangle. \tag{7}$$

The total wave function is written as $|\psi_{nS}^F\rangle = \psi_{nS}(r) \otimes |F\rangle$, where the spatial wave functions are

$$\begin{aligned} \psi_{1S}(r) &= \frac{1}{\sqrt{\pi a_0^3}} e^{-r/a_0}, \\ \psi_{2S}(r) &= \frac{1}{\sqrt{32\pi a_0^3}} \left( 2 - \frac{r}{a_0} \right) e^{-r/(2a_0)}, \end{aligned} \tag{8}$$

with $a_0$ being the Bohr radius. The expectation value of $V_i$ then takes the form

$$\langle V_i \rangle = \int |\psi_{1S/2S}(r)|^2 \langle F | V_i | F \rangle \, d^3 r. \tag{9}$$

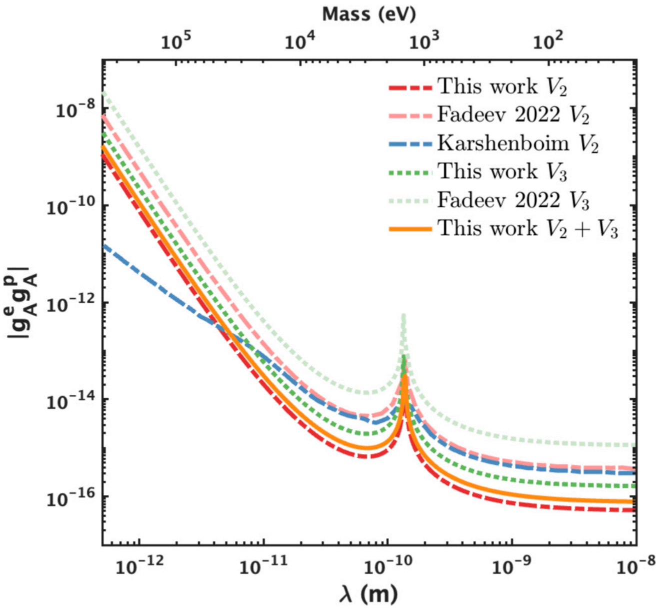


FIG. 1. Constraints on the coupling constants product $g_A^e g_A^p$. The results from this work are shown as the dark dash-dotted red, dark dotted green, and yellow solid curves for $V_2$, $V_3$, and $V_2 + V_3$, respectively, together with the results from Fadeev *et al.* [9] (light dash-dotted red and light dotted green curves) and Karshenboim [6] (dash-dotted blue curve).

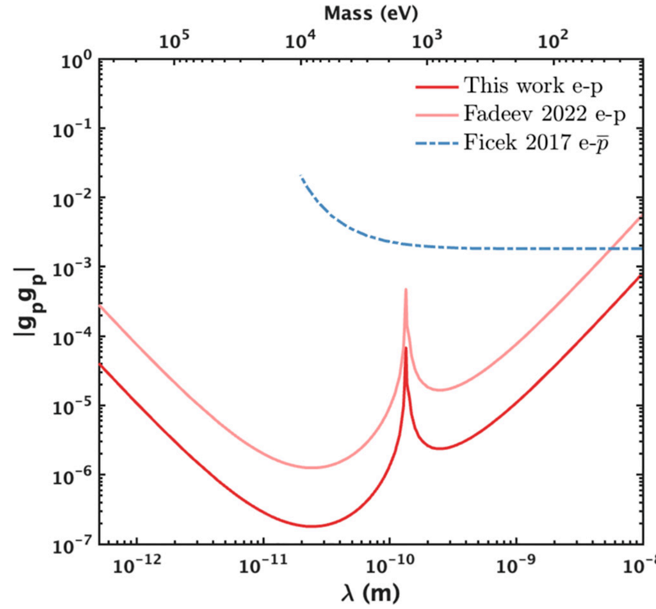


FIG. 2. Constraints on the coupling constants products $g_p^e g_p^p$ and $g_p^e g_p^{\bar{p}}$ coming from the study of $V_3$. The results for *e-p* come from this work (dark solid red) and Fadeev *et al.* [9] (light solid red), while the constraints for *e-$\bar{p}$* are from Ficek *et al.* [8] (dash-dotted blue curve).

As an example, consider the combined $V_2 + V_3$ potential for the vector-vector (VV) coupling, expressed in natural units ($\hbar = c = 1$),

$$\begin{aligned}
&\langle \psi_{1S}^{F=1} | (V_2 + V_3)|_{\mathrm{VV}} | \psi_{1S}^{F=1} \rangle \\
&\quad = g_V^e g_V^p \left( -\frac{2}{3\pi m_e m_p} \right) \frac{k^4 (M+k)}{(M+2k)^2}, \\
&\langle \psi_{2S}^{F=1} | (V_2 + V_3)|_{\mathrm{VV}} | \psi_{2S}^{F=1} \rangle \\
&\quad = g_V^e g_V^p \frac{1}{48\pi m_e m_p} k^3 \left[ \frac{M^2 (2M^2 + k^2)}{2(M+k)^4} - 1 \right],
\end{aligned} \tag{10}$$

where $k = 1/a_0$ and $M$ is the new boson mass. For the $|F = 0\rangle$ state, the expectation values are equal to $-3$ times those of the corresponding $|F = 1\rangle$ state. Additional expressions for other potentials can be found in the Appendix of Ref. [9].

Finally, the exotic energy shift $\Delta E_{D_{21}}^{\mathrm{Exotic}}$ can be expressed as the product of a boson-mass–dependent factor $C(M)$ and a coupling constant product $g^e g^p$,

$$|g^e g^p| \leqslant \frac{|\Delta D|}{|C(M)|}, \tag{11}$$

where $C(M) = \frac{1}{3\pi m_e m_p} [\frac{k^3 M^2 (2M^2+k^2)}{(M+k)^4} + \frac{8k^4 (M+k)}{(M+2k)^2} - 2k^3]$ and $\Delta D$ is the maximum allowed deviation provided in Table I. Alternatively, one may express the constraint as a function of $\lambda$ using $M = 1/\lambda$.

## III. RESULTS AND DISCUSSION

In Figs. 1–3, we present our results based on the latest theoretical framework, in comparison with those also derived from hydrogen spectroscopy but relying on earlier experimental and theoretical data from Ref. [9] as well as others [6,8]. They are presented as functions of the interaction range $\lambda$ (shown on the bottom $x$ axis with corresponding new spin-1 boson mass $M$ presented on the top $x$ axis) denoting the lower bound of the excluded region.

For the axial-vector–axial-vector interaction $g_A g_A$, our constraints (red solid line) obtained from studying $(V_2 + V_3)|_{AA}$ are the most stringent for $\lambda > 5 \times 10^{-12}$ m. It should be emphasized that our primary interest lies in the coupling

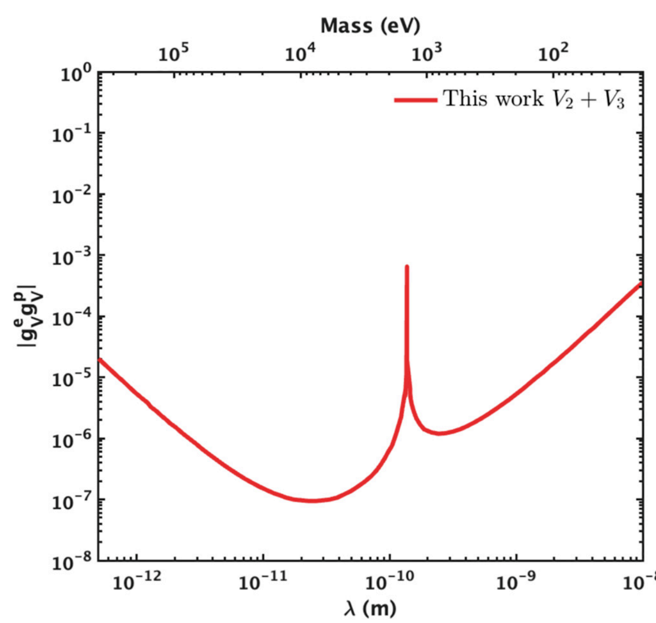


FIG. 3. Constraints on the coupling constants product $g_V^e g_V^p$.

coefficients $g_A^e g_A^p$. Therefore, it is essential to combine the $V_2|_{AA}$ and $V_3|_{AA}$ terms, as well as other terms that contribute to the axial-vector–axial-vector type of coupling (see Refs. [12,13,46]), whenever possible. In our case here, the combination yields a weaker constraint compared to the one that depends only on $V_2|_{AA}$ because the calculated $C(M)$ values from $V_2|_{AA}$ and $V_3|_{AA}$ have opposite signs. An intuitive understanding is that the exotic interactions associated with $V_2|_{AA}$ and $V_3|_{AA}$ would shift the value of $D_{21}$ in opposite directions. In some cases where the constraint lines obtained from $V_2|_{AA}$ and $V_3|_{AA}$ intersect, the corresponding contributions may completely cancel, causing the combined constraint to exhibit a divergence peak similar to the spike features shown in our figures. The spike feature of the constraints lines near $\lambda = 1.4 \times 10^{-10}$ m is due to a cancellation in the denominator of Eq. (11), i.e., $C(M) = 0$. Note that Ref. [9] originally obtained constraints on $g_A g_A$ by studying $V_2 + V_3$. Here, we redo the calculation and extract the constraints for $V_2|_{AA}$ and $V_3|_{AA}$ for the purpose of comparison. Karshenboim [6] combined the constraints based on $1S$ hfs and $D_{21}$ from hydrogen and studied $V_2$; thus the $V_2|_{AA}$ result extracted from Ref. [9] is the same as in Karshenboim [6] in the range of $\lambda > 10^{-11}$ m.

Additional constraints for $g_A^e g_A^p$ in the range $10^3 < \lambda < 10^{11}$ m can be found in Refs. [47,48] where exotic interactions between spin-polarized geoelectrons—based on the pyrolite model for Earth's electron spin distribution—and protons in a laboratory source were investigated. It is noted that Karshenboim [6] (dash-dotted blue curve) still provides the most stringent constraints for the range $\lambda < 4 \times 10^{-12}$ m. Possible improvements will be discussed in our forthcoming work.

Regarding the pseudoscalar-pseudoscalar interaction $g_p g_p$, our results (red solid line) set the most stringent constraints. Reference [9] previously provided the only constraints for exotic interactions between $e$-$p$. We present another result for $e$-$\overline{p}$ based on antiprotonic helium [8] for comparison.

For the vector-vector interaction $g_V g_V$, we present the constraints obtained by studying Eq. (5). As mentioned in the recent review [13], while current constraints are approximately inferred from $V_3$, no existing result has addressed the combination $V_2 + V_3$, except our recent study on spin-spin coupling in tritium deuteride (DT) [49]. We emphasize this point to draw the community's attention to the importance of further studies focusing on $V_2 + V_3$ [Eq. (5)] for vector-vector–type exotic interactions.

In summary, we have obtained improved constraints on electron-proton exotic interaction couplings $g_A g_A$, $g_p g_p$, and $g_V g_V$. Looking ahead, Bullis *et al.* [15] may achieve an additional tenfold improvement in precision by increasing the size of their setup [50], which would correspondingly further tighten the constraints on exotic electron-proton interactions.

*Note added.* Note that we present the 90% confidence level (CL) results in the figures of this work, as the other results used for comparison are given at the same level. However, following the suggestions made in the review [13], we also calculated the 95% CL results using Eq. (1), obtaining $\Delta D = 0.0170$ kHz. The 95% CL results are available online [51] and are also included in the fifth force dataset [52].


## ACKNOWLEDGEMENTS

The authors acknowledge helpful discussions with Mikhail G. Kozlov. This research has been supported in part by the Cluster of Excellence "Precision Physics, Fundamental Interactions, and Structure of Matter" (PRISMA++ EXC 2118/2) funded by the German Research Foundation (DFG) within the German Excellence Strategy (Project ID 390831469), the COST Action within the project COSMIC WISPers (Grant No. CA21106), and the Deutsche Forschungsgemeinschaft (DFG, German Research Foundation) in the framework to the collaborative research center "Defects and Defect Engineering in Soft Matter" (SFB1552) under Project No. 465145163. F.F. acknowledges the support of the Austrian Science Fund (FWF) via Project No. P 36455.


## DATA AVAILABILITY

The data that support the findings of this article are openly available [51].


[1] M. S. Safronova, D. Budker, D. DeMille, Derek F. Jackson Kimball, A. Derevianko, and C. W. Clark, Rev. Mod. Phys. **90**, 025008 (2018).

[2] M. Jiao, M. Guo, X. Rong, Y.-F. Cai, and J. Du, Phys. Rev. Lett. **127**, 010501 (2021).

[3] W. Ji, W. Li, P. Fadeev, F. Ficek, J. Qin, K. Wei, Y.-C. Liu, and D. Budker, Phys. Rev. Lett. **130**, 133202 (2023).

[4] Z. Xu, X. Heng, G. Tian, D. Gong, L. Cong, W. Ji, D. Budker, and K. Wei, Phys. Rev. Lett. **134**, 181801 (2025).

[5] B. R. Heckel, W. A. Terrano, and E. G. Adelberger, Phys. Rev. Lett. **111**, 151802 (2013).

[6] S. G. Karshenboim, Phys. Rev. A **83**, 062119 (2011).

[7] F. Ficek, Derek F. Jackson Kimball, M. G. Kozlov, N. Leefer, S. Pustelny, and D. Budker, Phys. Rev. A **95**, 032505 (2017).

[8] F. Ficek, P. Fadeev, V. V. Flambaum, D. F. Jackson Kimball, M. G. Kozlov, Y. V. Stadnik, and D. Budker, Phys. Rev. Lett. **120**, 183002 (2018).

[9] P. Fadeev, F. Ficek, M. G. Kozlov, D. Budker, and V. V. Flambaum, Phys. Rev. A **105**, 022812 (2022).

[10] J. E. Moody and F. Wilczek, Phys. Rev. D **30**, 130 (1984).

[11] B. A. Dobrescu and I. Mocioiu, J. High Energy Phys. 11 (2006) 005.

[12] P. Fadeev, Y. V. Stadnik, F. Ficek, M. G. Kozlov, V. V. Flambaum, and D. Budker, Phys. Rev. A **99**, 022113 (2019).

[13] L. Cong, W. Ji, P. Fadeev, F. Ficek, M. Jiang, V. V. Flambaum, H. Guan, D. F. Jackson Kimball, M. G. Kozlov, Y. V. Stadnik, and D. Budker, Rev. Mod. Phys. **97**, 025005 (2025).

[14] L. Cong, F. Ficek, P. Fadeev, Y. V. Stadnik, and D. Budker, arXiv:2503.07161.

[15] R. G. Bullis, C. Rasor, W. L. Tavis, S. A. Johnson, M. R. Weiss, and D. C. Yost, Phys. Rev. Lett. **130**, 203001 (2023).

[16] S. Weinberg, Phys. Rev. Lett. **40**, 223 (1978).

[17] F. Wilczek, Phys. Rev. Lett. **40**, 279 (1978).

[18] J. E. Kim, Phys. Rev. Lett. **43**, 103 (1979).

[19] A. R. Zhitnitsky, Yad. Fiz. **31**, 497 (1980) [Sov. J. Nucl. Phys. **31**, 260 (1980)].
[20] M. A. Shifman, A. I. Vainshtein, and V. I. Zakharov, Nucl. Phys. B **166**, 493 (1980).
[21] M. Dine, W. Fischler, and M. Srednicki, Phys. Lett. B **104**, 199 (1981).
[22] J. Jaeckel and A. Ringwald, Annu. Rev. Nucl. Part. Sci. **60**, 405 (2010).
[23] A. Arvanitaki, S. Dimopoulos, S. Dubovsky, N. Kaloper, and J. March-Russell, Phys. Rev. D **81**, 123530 (2010).
[24] P. Langacker, Rev. Mod. Phys. **81**, 1199 (2009).
[25] L. B. Okun, Zh. Eksp. Teor. Fiz. **83**, 892 (1982); JETP **56**, 502 (1982).
[26] B. Holdom, Phys. Lett. B **166**, 196 (1986).
[27] T. Appelquist, B. A. Dobrescu, and A. R. Hopper, Phys. Rev. D **68**, 035012 (2003).
[28] B. A. Dobrescu, Phys. Rev. Lett. **94**, 151802 (2005).
[29] J. Preskill, M. B. Wise, and F. Wilczek, Phys. Lett. B **120**, 127 (1983).
[30] L. F. Abbott and P. Sikivie, Phys. Lett. B **120**, 133 (1983).
[31] M. Dine and W. Fischler, Phys. Lett. B **120**, 137 (1983).
[32] Y. K. Semertzidis and S. Youn, Sci. Adv. **8**, eabm9928 (2022).
[33] F. Chadha-Day, J. Ellis, and D. J. Marsh, Sci. Adv. **8**, eabj3618 (2022).
[34] D. F. Jackson Kimball and K. van Bibber (eds.), *The Search for Ultralight Bosonic Dark Matter* (Springer International Publishing, Cham, 2023).
[35] R. D. Peccei and H. R. Quinn, Phys. Rev. D **16**, 1791 (1977).
[36] R. D. Peccei and H. R. Quinn, Phys. Rev. Lett. **38**, 1440 (1977).
[37] M. I. Eides, H. Grotch, and V. A. Shelyuto, Phys. Rep. **342**, 63 (2001).
[38] S. G. Karshenboim and V. G. Ivanov, Phys. Lett. B **524**, 259 (2002).
[39] S. G. Karshenboim and V. G. Ivanov, Eur. Phys. J. D. **19**, 13 (2002).
[40] V. A. Yerokhin and U. D. Jentschura, Phys. Rev. Lett. **100**, 163001 (2008).
[41] S. G. Karshenboim, Phys. Rep. **422**, 1 (2005).
[42] C. Quint, F. Heiße, J. Jaeckel, L. Leimenstoll, C. H. Keitel, and Z. Harman, arXiv:2506.03274v1.
[43] S. G. Karshenboim and V. G. Ivanov, Can. J. Phys. **83**, 1063 (2005).
[44] S. G. Karshenboim, S. I. Eidelman, P. Fendel, V. G. Ivanov, N. N. Kolachevsky, V. A. Shelyuto, and T. W. Hänsch, Nucl. Phys. B **162**, 260 (2006).
[45] H. Hellwig, R. F. C. Vessot, M. W. Levine, P. W. Zitzewitz, D. W. Allan, and D. J. Glaze, IEEE Trans. Instrum. Meas. **19**, 200 (1970).
[46] P. Fadeev, Neue Eichbosonen und wo Man sie Findet, Master's thesis, Johannes Gutenberg-Universität Mainz, Helmholtz-Institut Mainz, 2018.
[47] L. Hunter, J. Gordon, S. Peck, D. Ang, and J.-F. Lin, Science **339**, 928 (2013).
[48] L. R. Hunter and D. G. Ang, Phys. Rev. Lett. **112**, 091803 (2014).
[49] L. Cong, D. F. J. Kimball, M. G. Kozlov, and D. Budker, arXiv:2408.15442.
[50] M. Rini, Physics **16**, s72 (2023).
[51] L. Cong, Improved constraints on exotic electron-proton interactions in hydrogen [Data set], Zenodo (2025), https://doi.org/10.5281/zenodo.15492351.
[52] L. Cong, Lei-Cong/Spin-Dependent-5th-Force-Limits: v3.2, Zenodo (2025), https://doi.org/10.5281/zenodo.14572652.